Solution structures of the 9-ketone and 9,12-hemiacetal forms of erythromycin A in 90% H_2O as determined by NMR and molecular modelling

Fernando Commodari,*[,a] George E. Sclavos,†[,a] Abdesslem Khiat[b] and Yvan Boulanger[b]

[a] *Chemistry Department, Long Island University, One University Plaza, Brooklyn, NY 11201, USA*
[b] *Hôpital Saint-Luc, Centre Hospitalier de l'Université de Montréal, 1058 St. Denis, Montréal, Québec, Canada, H2X 3J4*

The one-dimensional proton NMR spectrum of an aqueous solution (90% H_2O, 10% ^2H_2O, in phosphate buffer, pH 7.0) of 10 mM erythromycin A is assigned using double quantum filtered correlation spectroscopy (DQFCOSY) and total correlation spectroscopy (TOCSY) spectra. These assignments are then used to determine spatial relationships between the protons obtained from the rotating-frame Overhauser enhancement spectroscopy (ROESY) spectrum. Molecular modelling, with the NMR derived NOE distance constraints from the ROESY spectrum, is used to determine the solution structures of the 9-ketone and the 9,12-hemiacetal forms of the compound. The structure obtained for the ketone is consistent with previous studies (in other solvents), except for some interesting variations in the sugar moieties. For both the 9-ketone and 9,12-hemiacetal, the aglycone ring is found to be primarily 'folded out', in a fully staggered Perun type conformation and the sugar moieties are all found to be in the boat conformation and parallel up at the 3 and 5 aglycone ring positions. This study is the first to provide a solution structure for the hemiacetal, which is found to be in equilibrium with the ketone, and the first to look at erythromycin A and its 9,12-hemiacetal tautomer in 90% H_2O at physiological pH. The ratio of 9-ketone to 9,12-hemiacetal is found to be 5:1. Peaks for the 6,9-hemiacetal are observed at very low intensity.

Introduction

Erythromycin A (**1**) is a member of the macrolide group of antibiotics. It consists of a 14-membered polyfunctionalized lactone (aglycone) ring with cladinose and desosamine sugar rings on C3 and C5, respectively. McGuire and associates[1] first isolated **1** in 1952.

Erythromycin is one of the safest drugs ever developed, rarely causing side effects. Erythromycin is useful in treating most Gram-positive bacteria and some Gram-negative bacteria. Erythromycin is effective against specific microorganisms such as *Streptococcus pneumoniae*, *Haemophilus influenzae*, *Chlamydia*, *Coxiella burnetii*, *Nocardia* and *Actinomyces*. Erythromycin A is the drug of choice for Legionnaire's disease, diarrhea caused by *Campylobacter Jejuni* and infections caused by Mycoplasma.[2]

The ring-chain tautomers (tautomers) of **1** in various solvents {$C[^2H]Cl_3$, ^2H_2O, $[^2H_6]$DMSO, $C_5[^2H_5]N$, $(C[^2H_3])_2CO$, $(C[^2H_3])_2SO$, $C[^2H_3]O[^2H]$, $(C[^2H_3])_2NC[^2H]O$} have been studied extensively by NMR spectroscopy.[3–6]§ Everett and Tyler[3] were the first to complete an unambiguous assignment of the ^1H and ^{13}C spectra of **1** in $C[^2H]Cl_3$. Everett and Tyler[4] were also the first to determine that a major tautomer of **1** is in fast equilibrium with a minor tautomer with the difference in structure occurring in the C2 to C9 region. Everett *et al.*[5] determined that **1** and a majority of its derivatives exist in two major aglycone ring conformations, called A and B. Conformation A is based on the X-ray crystallographic structure of erythromycin hydroiodide dihydrate and conformation B is based on the X-ray crystallographic structure of (9*S*)-9-*N*,11-*O*-[2-(2-methoxyethoxy)ethylidene]erythromyclamine A. The major difference between conformations A and B is that in the so called 'folded-in' aglycone ring conformer B there is an inward folding of the C3 to C5 section such that H3 and H11 are closer in the conformational space. In the 'folded-out' conformation A, H4 and H11 are closer.

Ager *et al.*[7] completely and unambiguously assigned the ^{13}C spectrum of **1** on the basis of the ^{13}C DEPT[8,9] and INADEQUATE[10] spectra. Barber *et al.*[11] completely assigned the ^1H and ^{13}C spectra of **1** in ^2H_2O and $[^2H_6]$DMSO. They concluded that **1** exists as a hemiacetal with the bridge occurring between C9 and C12 based on β-^2H shift studies.[12,13] They also determined that the ratio of 9-ketone to 9,12-hemiacetal is *ca.* 5:2 in ^2H_2O and 5:1 in $[^2H_6]$DMSO.

Steinmetz *et al.*[14] disputed the results of Barber *et al.*[11] with respect to erythromycin A by stating that the 4 Å distance between C9 and C12 (determined from the crystal structure of **1**) would require significant conformational changes in the macrolide ring to reduce this distance for the hemiacetal bridge to occur there. Steinmetz *et al.*[14] suggested instead that the hemiacetal bridge should occur between C6 and C9.

Everett *et al.*[6] determined that bridging occurred between carbons 9 and 12 and carbons 6 and 9, as shown. They completed NMR studies on **1** using six different solvents. They concluded that the location of bridging is directly related to the polarity of the solvent. The greater the polarity of the solvent, the greater the percentage of the 9,12-hemiacetal compared to the 6,9-hemiacetal.

The location of the hemiacetal bridge is of special importance to the study of erythromycin A because bacterial

† Part of this work comprised a Westinghouse Science Project carried out by G. E. S. at Midwood High School, Brooklyn, NY 11210, USA.
‡ The following acronyms for NMR techniques are used in this paper. Distortionless enhancement by polarisation transfer (DEPT), incredible natural abundance double quantum transfer experiment (INADEQUATE), double quantum filtered correlation spectroscopy (DQFCOSY), total correlation spectroscopy (TOCSY), rotating-frame Overhauser enhancement spectroscopy (ROESY), heteronuclear multiple quantum coherence (HMQC), heteronuclear correlation spectroscopy (HETCOR).

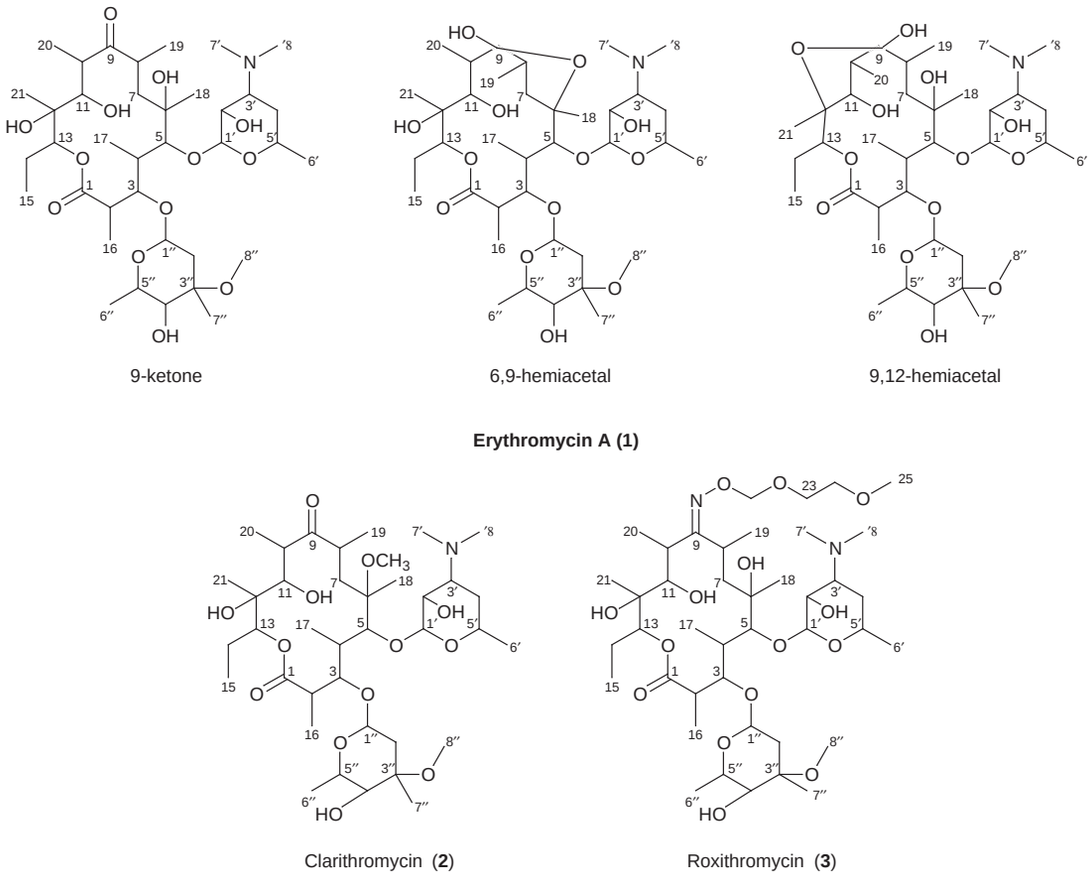

Chemical structures of erythromycin A (**1**) in the ketone, 6,9-hemiacetal and 9,12-hemiacetal forms as well as the structures of clarithromycin (**2**) and roxithromycin (**3**) analogues

resistance to the drug is obtained through the hemiacetal. This antibiotic works by binding to the 50S subunit of the 70S bacterial ribosome.[2] The ketone binds to the 50S subunit, while the hemiacetal does not.[15] Many research groups have created various analogues of **1** hoping to eliminate the hemiacetal tautomer and to improve drug efficacy. Derivatives of **1** have been studied using NMR by Steinmetz *et al.*,[14] Awan *et al.*[16] and Gharbi-Benarous *et al.*[17,18] Steinmetz *et al.*[14] completely assigned the ^{1}H spectrum of clarithromycin (6-methoxy-erythromycin) **2**, in ^2H_2O and C[^{2}H]Cl$_3$. Clarithromycin can form a hemiacetal bridge between carbons 9 and 12. However, Steinmetz *et al.*[14] determined that **2** exists primarily in the ketone form in C[^{2}H]Cl$_3$ solution. Awan *et al.*[16] completely and unambiguously assigned the ^{1}H and ^{13}C spectra of **2**, in ^2H_2O and C[^{2}H]Cl$_3$. Gharbi-Benarous *et al.*[17,18] studied another derivative of **1**, roxithromycin **(3)**, in C[^{2}H]Cl$_3$ and C[^{2}H$_3$]O[^{2}H]. Antibiotic **3** differs from **1** by the replacement of the carbonyl group on C9 with a *O*-(2,5-dioxahexyl) oxime group. The *O*-(2,5-dioxahexyl) oxime group on C9 prevents formation of the hemiacetal tautomer. They also concluded that the oxygen in the *O*-(2,5-dioxahexyl) oxime group forms hydrogen bonds with the hydrogens of the hydroxy groups on C6 and C11, leading to a globular molecule. They also determined that in C[^{2}H]Cl$_3$ and C[^{2}H$_3$]O[^{2}H] solvents, both sugars are in the chair conformation as in **1**,[4] but the aglycone ring of **3** is 'folded in', unlike in **1**.[5] When the biological activities of **3** and **1** are compared,[19] a better activity is found *in vitro* for **1** but **3** is a far superior antibiotic *in vivo*. The differences[19] have been attributed to a greater penetration of **3** rather than **1** into all tissues. It is not clear if this is related to structural differences.

Due to the importance of the location of the hemiacetal bridge for bacterial resistance to erythromycin A, the present study investigates the solution structure of **1** in 90% H_2O by NMR and molecular modelling. This is the first study to examine the conformation of **1** in 90% H_2O at physiological pH. The immediate goals are to determine the major tautomers and the position(s) of bridge formation, in view of the solvent dependent differences seen in the past literature for erythromycin A and its derivatives. In addition, it is of interest to see if the aglycone ring is folded in or out. Once the 3D structures are determined for the major tautomers in 90% H_2O, structure–activity studies can be carried out to determine the key structural elements required for activity in the design of new peptidomimetic analogues for clinical trials against Gram-positive bacteria. An understanding of the solution structures of the related tautomers at physiological conditions is a prerequisite to the rational design of new drugs void of bacterial resistance. The goal is to correlate structure to activity. First, one would like to determine the structure of erythromycin A and then relate its activity to its structure leading to modified analogues and new drug candidates. Although obtaining ribosomal binding information for erythromycin A may be useful, as long as one has a point of reference or control, then one can rationally proceed to design new drug candidates based on traditional structure–activity relations. As long as one has a point of reference for the parent molecule, this being a given solvent and other experimental conditions, then one may relate changes in structure to changes in *in vitro* or *in vivo* activity of the derivative drug.

Results

Fig. 1 shows the 1D spectrum of **1** in 90% water and 10% deuterium oxide. Table 1 shows the ^{1}H chemical shifts and nuclear Overhauser effect (NOE) connectivities obtained, from the 1D and 2D data sets of the two major tautomers of **1** (9-ketone and 9,12-hemiacetal) in 90% H_2O.

Initial assignments were made using pattern recognition from previous work by Steinmetz *et al.*[14] and Barber *et al.*[11] These sequential assignments were then confirmed using a DQF-

Table 1 ^{1}H chemical shifts and connectivities for erythromycin[a]

	δ_H		Coupling	
Proton	Ketone	9,12-Hemiacetal	DQFCOSY	ROESY
2	3.01	2.99	16, 3	17, 16, 4a′
3	3.79	3.89	2	16, 13, 4a′, 10, 5, *11*, 1″, **1′**
4	1.97	2.16	17	17, 11, 7a, ***10***
5	3.51	3.53		6′, 6″, 1′, 5″, **5′**, 3, 18
6OH	1.73		18	13
7a	1.90	1.85	8	10, 18, 4, 2e″
7e	1.56	1.28	8	7′8′, 14a
8	2.69	1.52	19, 7e, 7a	4a′ 18, 19
10	3.23	2.18	11, 20	17, 16, 18, 7a, 3, 3′, ***4***, **20**
11	3.74	3.96	10	4, ***18***, ***3***
12OH	2.19		21	
13	5.00			6OH, 3, 15
14a	1.77	1.99	15	18, 7e, *15*
14e	1.50	1.83	15	
15	0.78	0.82	15a, 14e	13, ***14a***
16	1.17	1.17	2	3, 10, 2, 2a″
17	1.03	1.03	4	1′, 1″, 10, 2, 4
18	1.34	1.23	6OH	*11*, 5, 8, 7a, 14a, 10
19	1.13	1.13	8	8
20	1.05	1.09	10	**10**
21	1.21	1.31	12OH	
′sugar				
1′	4.55	4.47	2′	3, 5, 17, 5″
2′	3.46	3.43	1′	12OH, 4a′, **7′8′**
3′	3.41	3.41	4a′, 4e′	10
4′a	2.05	2.08	3′	3, 2′, 7′8′, 8, **2e″**, 2
4′e	1.44	1.42	3′, 5′	
5′	3.85	3.92	6′, 4e′	6′, **5**
6′	1.23	1.27	5′	5, 5′, 5″
7′8′	2.81	2.79		7e, 4a′, **2′**
″sugar				
1″	4.86			17, 7″, 3, **2e″**
2″a	2.41	2.41		4″, 2e″, 16
2″e	1.61	1.58		7a, 2a″, 4″, 7″, **1″**, **4a′**
4″	3.16	3.19	5″	2a″, 2e″, 7″
5″	4.07	4.12	6″, 4″	3, 6′, 6″, 5, 1′
6″	1.31	1.29	5″	5, 5″
7″	1.19	1.18		1″, 4″, 2e″

[a] Italicized font denotes 9,12-hemiacetal to ketone coupling, bold font denotes exclusive 9,12-hemiacetal coupling and regular font denotes couplings for both the ketone and the hemiacetal.

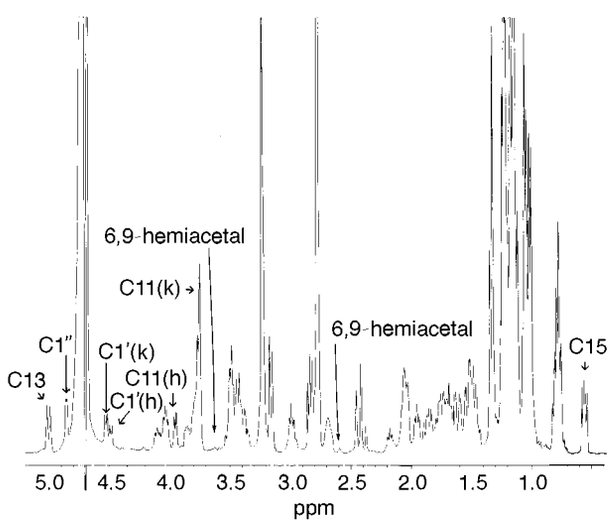

Fig. 1 400 MHz ^{1}H NMR spectrum of 10 mM erythromycin prepared in 90% H_2O and 10% ^2H_2O with phosphate buffer at pH 7.0. Selected peaks are assigned [9-ketone (k), 9,12- (h) and 6,9-hemiacetal].

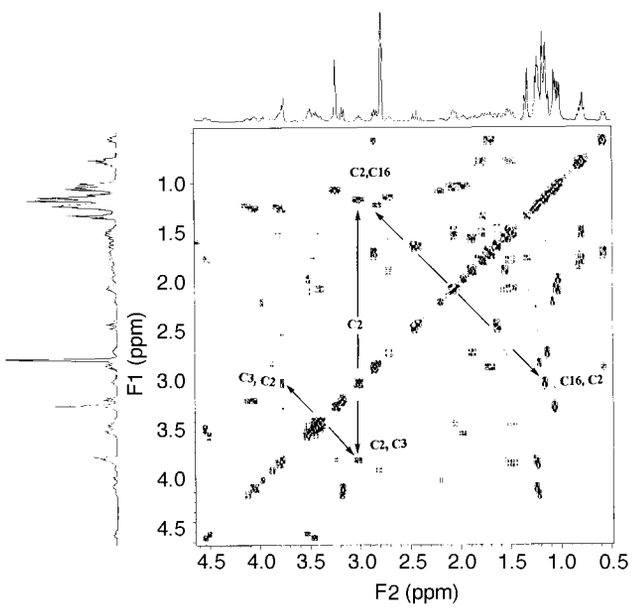

Fig. 2 DQFCOSY spectrum of **1**. The couplings between protons on C2 and C3 and C2 and C16 are shown.

COSY spectrum (Fig. 2). The ketone protons on C3, C7a, C7e, C14a, C14e, C15, C17, C18, C21, C1′, C6″ were assigned using this method. The 9,12-hemiacetal protons on C3, C4, C7a, C7e, C14e, C15, C18, C19, C20, C6′, C4″ and C6″ were also assigned using this method. The relevant DQFCOSY connectivities for both the ketone and the 9,12-hemiacetal are shown in Table 1. The ketone protons on C2, C4, C6OH, C8, C10, C11, C16, C12OH, C19, C20, C2′, C3′, C4a′, C4e′, C6′, C4″ and C5″ were assigned using the DQFCOSY as were the 9,12-hemiacetal protons on C2, C8, C10, C11, C14a, C16, C17,

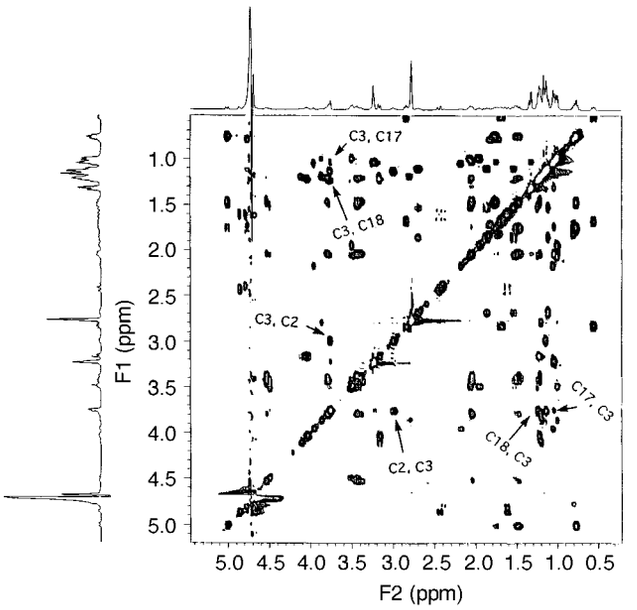

Fig. 3 TOCSY spectrum of **1**. All C3 couplings are shown as examples of how coupling was used to make through bond assignments.

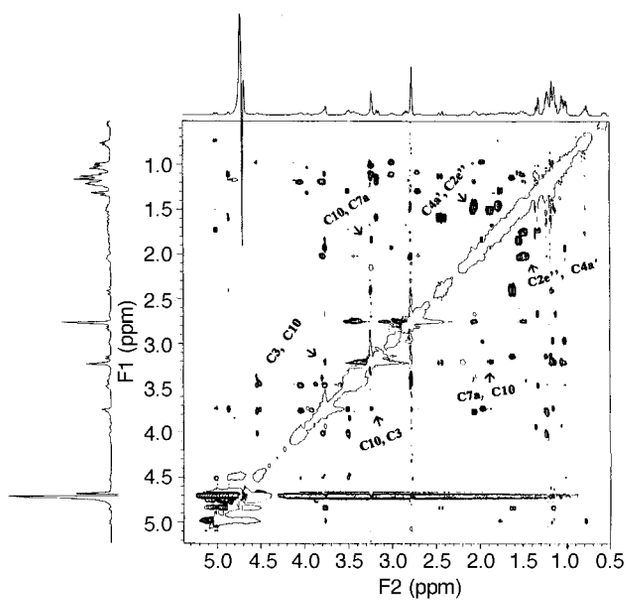

Fig. 4 ROESY spectrum of **1**. Examples of large (C4a′, C2e″) and medium (C10, C7a and C3, C10) dipolar distance constraints are identified.

C21, C1′, C2′, C3′, C4a′, C4e′, C5′ and C5″. The relevant couplings are shown in Table 1. The TOCSY connectivities were used in assigning protons on C5, C7′8′, C2a″, C2e″, C7″ for both the ketone and the 9,12-hemiacetal (Fig. 3). The TOCSY was also used in assigning protons on C13 and C1″ for the ketone.

Table 2 provides the NOE constraints used for molecular modelling. The data were obtained from the 2D ROESY spectrum (Fig. 4) with the labels of 'S' for small (1.8–5 Å), 'M' for medium (1.8–4 Å), and 'L' for large (1.8–3 Å) dipolar distance constraints. One Å was added to the NOE constraints for degenerate protons on a methyl or methylene carbon due to the creation of a pseudo atom for molecular modelling.

Shown in Fig. 5 is a 1D NOE difference ^{1}H spectrum resulting from the excitation of the proton on C5″ of the cladinose sugar unit of erythromycin A at 4.12/4.07 ppm (ketone/hemiacetal). NOEs are seen at 4.61/4.58 (ketone/hemiacetal), 3.56/3.54, 3.21 (hemiacetal only) and 1.29/1.27 ppm corresponding, respectively, to protons attached to C1′, C5, C4′, C6′ and C6′. These

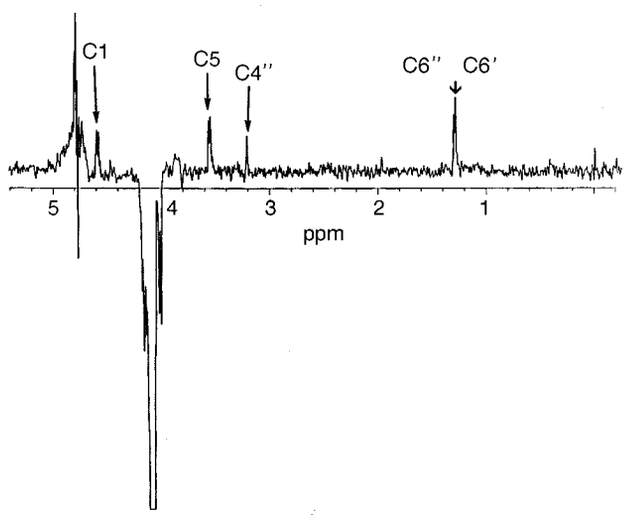

Fig. 5 A 1D NOE difference spectrum of **1** when the peak of H5″ at 4.12/4.07 ppm (ketone/9,12-hemiacetal) was irradiated. This spectrum contains the selective excitation of both the water resonance and the NOE.

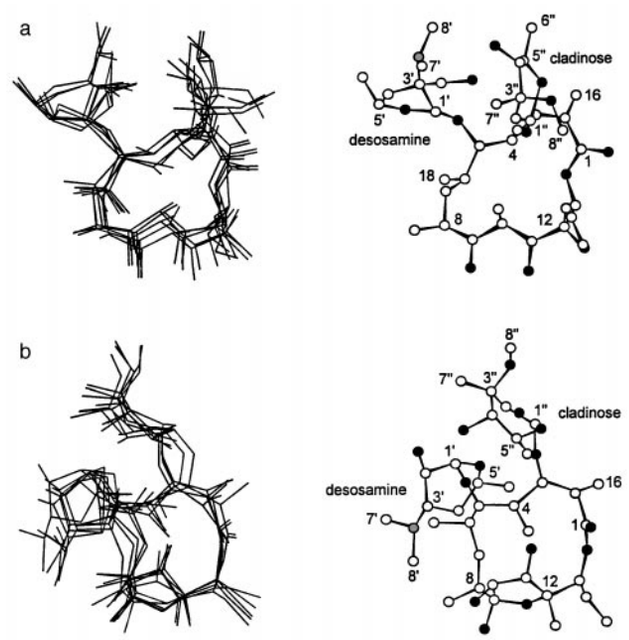

Fig. 6 (a) A superposition of 5 (out of 25) structures of the 9-ketone tautomer of **1** calculated by molecular modelling on the basis of NMR data. (b) A superposition of 5 (out of 25) structures of the 9,12-hemiacetal tautomer of **1** calculated by molecular modelling on the basis of NMR data. Ball and stick models of the 9-ketone and 9,12-hemiacetal are also shown with black, gray and white circles indicating, respectively, oxygen, nitrogen and carbon atoms.

dipolar couplings are consistent with the 2D ROESY data. Split peaks are seen for the 9-ketone and 9,12-hemiacetal tautomers.

Integration of protons on C11, with chemical shifts at 3.74 ppm for the ketone and 3.96 ppm for the 9,12-hemiacetal, indicates that the ketone to hemiacetal ratio is 5:1 in 90% H_2O and 10% ^2H_2O. This ratio is the same ratio as that determined for **1** in [$^2H_6$]DMSO by Barber *et al.*,[11] but different from their results in ^2H_2O (5:2 ratio).

Fig. 6(a) shows the superposition of 5 (out of 25) structures for the 9-ketone derived from the modelling with NOE constraints. The root mean square deviation (RMSD) value was 1.74 Å for a total of 25 structures. The current work determined the macrolide ring of the 9-ketone to be 'folded out' in the C3–C5 region (the mean H4 to H11 distance was found to be 1.96 Å) and to be flexible in the C6 to C9 region. The present study

Table 2 NOE constraints used in molecular modelling[a]

	2	3	4	5	6OH	7a	7e	8	9	9OH	10	11	11OH	12OH	13	14a	14e	15	16	17	18	19	20	21	1′	2′	2′OH	3′	4′a	4′e	5′	6′	7′8′	1″	2″a	2″e	4″	4″OH	5″	6″	7″	8″
2																S			L	L								S														
3				M							M	**M**			S				M						**S**,M			L						M								
4						S					M	L								M																						
5		M																			M				**M**					M	L							L	M		
6OH															S																											
7a			S								S										S													S							
7e																M																	M									
8																S					S	S						S														
9																																										
9OH																																										
10		M	M			S													L	L	S		**S**																		
11		**M**	L																		**S**																				
11OH																																										
12OH																										L																
13		S			S													S																							
14a							M											S			S																				
14e																																										
15															S	S																										
16	L	M									L																								S							
17	L		M								L														S									S								
18				M		S		S			S	**S**				S																										
19								S																																		
20											**S**																															
21																																										
1′		**S**,M		**M**																S																			M		
2′														L														S				L									
2′OH																																										
3′																																										
4′a	S	L						S																		S							M			L					
4′e																																										
5′				M																												L									
6′				L																										L									M		
7′8′							M																			L		M													
1″		M																		S															**M**				M		
2″a																			S																M	**M**					
2″e						S																						L					S	**M**	M		M				M	
4″																																				M	M					M	
4″OH																																										
5″				L																					S							**M**								L	
6″				M																												S									
7″																													M					M		M	L					
8″																																										

[a] Regular font denotes both 9-ketone and 9,12-hemiacetal couplings; bold font denotes exclusive 9,12-hemiacetal couplings.

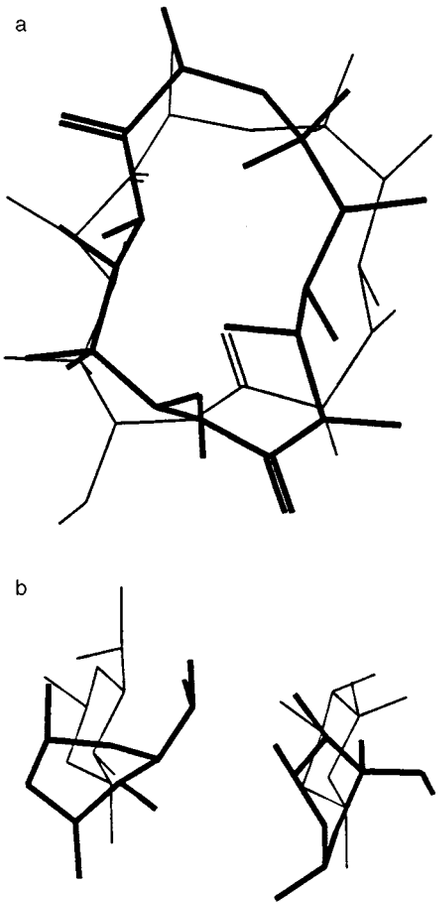

Fig. 7 (a) A comparison of the conformation of the aglycone ring as found in the present study (thick line) and in the study by Everett and Tyler (ref. 4) (thin line). (b) A comparison of the structures of the desosamine (on the left) and cladinose (on the right) sugars obtained in this study (thick line) as compared to the findings of Everett and Tyler (ref. 4) (thin line) based on their NOE constraints.

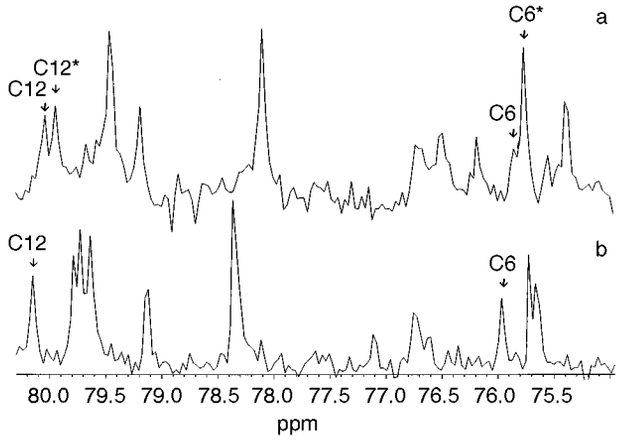

Fig. 8 ^{13}C β-^{2}H spectra of **1** in (a) 80:20 $^{2}H_2O$:H_2O and (b) 20:80 $^{2}H_2O$:H_2O. It is apparent that all of the shifts for the hydroxy groups are shifted upfield in (a), in addition to the appearance of 'extra' peaks due to upfield β-^{2}H shifts (indicated by an asterisk) for the peaks identified (by an arrow) as C6 and C12. In (b), C12 is seen at 80.15 ppm and C6 at 75.96 ppm. The peak for C9 was consistently seen as a singlet at 248.3 ppm in (a) and (b).

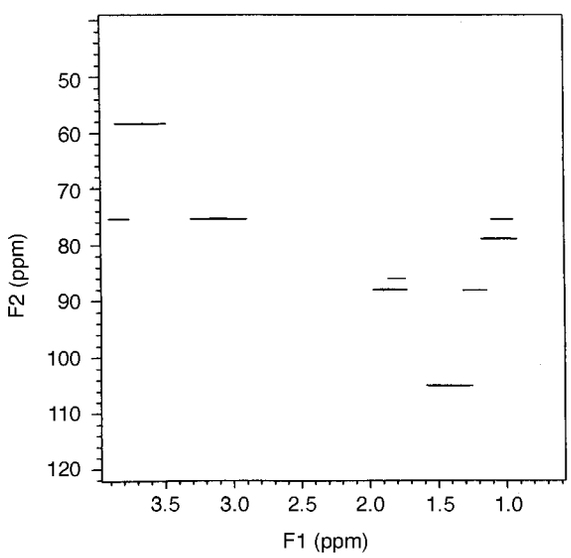

Fig. 9 A long range HETCOR of **1**

also determined that the cladinose and desosamine sugars were parallel up and found them to have the boat conformation rather than the chair conformation as in past studies.[4,17] This figure demonstrates the homology between the calculated structures. Fig. 6(b) shows the superposition of 5 (out of 25) structures for the 9,12-hemiacetal with a RMSD value of 1.67 Å for a total of 25 structures. The aglycone ring was determined to be conformationally flexible in the C6 to C9 region. Both the cladinose and desosamine sugars were determined to be in the boat conformation and parallel up, as in the ketone. This is the first study to determine the solution structure of the 9,12-hemiacetal. This figure demonstrates the homology between the calculated structures. Fig. 6 also provides ball and stick models of the 9-ketone and 9,12-hemiacetal.

Fig. 7(a) shows the conformation of the aglycone ring as found in the present study (thick line) and compared to that of Everett and Tyler[4] (thin line). In the present work, the aglycone ring was found to have a fully staggered Perun type[20,21] structure. Fig. 7(b) shows a comparison of the desosamine and cladinose sugars in this study (thick line) to the findings of Everett and Tyler[4] (thin line) based on their NOE constraints. In the present work, contrary to the sugar conformations of Everett and Tyler[4] on **1**, and Gharbi-Benarous *et al.*[17,18] on **3**, both the cladinose and desosamine sugar moieties showed boat conformations.

Fig. 8 shows the results of the ^{13}C β-^{2}H shift experiments. The bottom ^{13}C spectrum (b) is for 10 mM erythromycin A in 20:80 $^{2}H_2O$:H_2O. In the top spectrum (a) the same amount of erythromycin A was prepared in 80:20 $^{2}H_2O$:H_2O. It is apparent that all of the chemical shifts for carbons attached to hydroxy groups are displaced upfield in the top trace, in addition to the appearance of 'extra' peaks due to upfield β-^{2}H shifts (indicated by an asterisk) for the peaks identified (by an arrow) as C6 and C12. In the bottom trace, C12 is seen at 80.15 ppm and C6 at 75.96 ppm. The peak for C9 was consistently seen as a singlet at 248.3 ppm. Fig. 8 shows that both the 9,12-hemiacetal and the 6,9-hemiacetal are present in 80:20 $^{2}H_2O$:H_2O, as there are free hydroxy groups on C6 and C12 to undergo ^{2}H substitution leading to an upfield shift in the ^{13}C chemical shifts for these carbons. Not all of the peaks in the top trace were displaced in 80:20 $^{2}H_2O$:H_2O; those for carbons attached to hydroxy groups were displaced. Barber *et al.*[11] have noted that the spectra of **1** are sensitive to sample preparation and the experimental conditions. According to Barber *et al.*,[11] changes in chemical shift (in particular ^{13}C) of up to 0.1 ppm are observed from one spectrum to another even without discernible differences in pH or temperature of the sample. Clearly, in going from a mixture of 20:80 to 80:20 $^{2}H_2O$:H_2O, changes in chemical shift are to be expected in addition to β-^{2}H shift effects. C6 was assigned using a long range HETCOR. In Fig. 9, two long range couplings at 75.96 ppm on the carbon scale to 3.01 and 3.74 ppm on the proton scale are seen. The 3.01 ppm shift corresponds to protons on C2 and the 3.74 ppm shift corresponds to protons on C11. Based on previous ^{13}C[6–8]

Table 3 $^3J_{H-H}$ coupling constants (in Hz) for erythromycin

Coupled protons	$^3J_{H-H}$ [a]	$^3J_{H-H}$ [b]	$^3J_{H-H}$ [c]
H2–H3	7.9	9.5	9.4
H3–H4	1.5	1.5	1.5
H4–H5	6.9	7.5	7.7
H7a–H8	9.7	11.7	11.7
H7e–H8	3.8	2.4	2.5
H10–H11	1.2, **7.1**	1.3	1.3
H13–H14a	10.7	11.0	11.0
H13–H14e	2.3	2.4	2.4

[a] Bold font denotes the 9,12-hemiacetal form, regular font denotes the ketone form. Coupling constants were measured with a digital resolution of 0.5 Hz, after zero filling to 32 k. [b] Values from Everett and Tyler (see ref. 4) in deuterochloroform. [c] Values from Gharbi-Benarous *et al.* (see ref. 23).

assignments, the carbon peaks at 75.96 ppm could only be assigned to C6 or C13. There was also a coupling at 75.96 ppm on the carbon scale connecting to 1.03 ppm on the proton scale. The 1.03 ppm shift correlates to protons on C17, which are too far to be coupled to C13 in a long range HETCOR. Only C6 can experience a long range HETCOR coupling to protons on C2, C11 and C17.

Barber *et al.*[11] determined the hemiacetal bridge to be between C9 and C12 using the isotopic effect of β-^{2}H on ^{13}C NMR chemical shift values. Correlation of the ^{1}H chemical shifts with the ^{13}C shifts allowed for unequivocal assignment of the ^{1}H shifts for the 9-ketone and 9,12-hemiacetal. This data was used in the present study for some of the proton assignments as was a HMQC[22] (data not shown) and a long range HETCOR (Fig. 9).

Figs. 8 and 9 represent ^{13}C{^{1}H} detected (in a 5 mm diameter NMR tube) 1D and 2D NMR spectra using only 0.7 mL of 8 mM erythromycin. The two figures are included to reinforce the ^{1}H NMR findings. It was deemed important to have β-^{2}H shift studies with different levels of deuterium oxide to see the results and conclusively determine the locations of bridge formation.

Discussion

^{1}H resonance assignments (Table 1) were made for the 9-ketone, 9,12-hemiacetal and the 6,9-hemiacetal of erythromycin A. This is the first study to determine the solution structure of the 9,12-hemiacetal from distinct NOE couplings due to this tautomer. It was determined that the aglycone ring is primarily folded out and the cladinose and desosamine sugars are in the boat conformation and parallel up for the 9,12-hemiacetal and the 9-ketone.

The present work found the sugars to be in the boat conformation rather than in the chair conformation as was reported by Everett and Tyler[4] and Gharbi-Benarous *et al.*[18,23] For the desosamine sugar, NOE couplings were seen, in the present work for ^{1}Hs on C5 and C5′ (M), C4a′ and C8 (S), and C2′ and C4a′ (S). These couplings provide evidence for the boat conformation. None of these couplings were seen in the study completed by Everett and Tyler.[4] Couplings for ^{1}Hs on C3′ and C5′ (L), C1′ and C3′ (M), C1′ and C5′ (M), and C3 and C7′8′ (M) indicate chair conformation and were seen by Everett and Tyler[4] but not in the present work. For the cladinose sugar, Everett and Tyler[4] found a coupling of small intensity between ^{1}Hs on C2a″ and C4″. The present work found this coupling to be large. This indicates that they are closer in conformational space. For these two ^{1}Hs to be closer in the conformational space, the entire structure of the ring must change supporting the boat conformation rather than the chair.

The present work supports the finding of Barber *et al.*[11] that the hemiacetal bridge occurs mainly between C9 and C12. The chemical shifts found were primarily those for the 9-ketone and 9,12-hemiacetal. The large change in coupling (Table 3) between protons on C10 and C11 from the ketone (1.2 Hz $^3J_{H-H}$) to hemiacetal (7.1 Hz $^3J_{H-H}$) also supports the C9–C12 bridge formation leading to a large change in torsion angle. Furthermore, the ROESY derived NOE constraints for the hemiacetal lead to modelling of the C9–C12 bridged structures with very good homology (RMSD = 1.67 Å *vs.* 1.74 Å for the ketone) and no violations greater than 0.5 Å in the dipolar couplings obtained from the ROESY data. However, evidence is also seen in the 1D ^{1}H spectrum, Fig. 1, for the presence of the 6,9-hemiacetal tautomer with chemical shifts at 3.06, 3.63, 3.91 and 4.03 ppm and several other peaks not much above the baseline noise. All of these 6,9-hemiacetal peaks were much lower in intensity than any of the 9,12 peaks (see Table 1). ^{13}C β-^{2}H shift experiments, Fig. 8, also show the presence of all three tautomers at 80 : 20 ^2H_2O : H_2O.

Fig. 8 shows the results of the ^{13}C β-^{2}H shift experiments. The bottom ^{13}C spectrum (b) is for 10 mM erythromycin A in 20 : 80 ^2H_2O : H_2O. In the top spectrum (a) the same amount of erythromycin A was prepared in 80 : 20 ^2H_2O : H_2O. It is apparent that all of the chemical shifts for the carbons attached to hydroxy groups are displaced upfield in the top trace, in addition to the appearance of 'extra' peaks due to upfield β-^{2}H shifts (indicated by an asterisk) for the peaks identified (by an arrow) as C6 and C12. In the bottom trace, C12 is seen at 80.15 and C6 at 75.96 ppm. The peak for C9 was consistently seen as a singlet at 248.3 ppm. Fig. 8 shows that both the 9,12-hemiacetal and the 6,9-hemiacetal are present in 80 : 20 ^2H_2O : H_2O, as there are free hydroxy groups on C6 and C12 to undergo ^{2}H substitution leading to an upfield shift in the ^{13}C chemical shifts for these carbons. This is possible only if there are C6 and/or C12 hydroxy groups not bridged in a hemiacetal structure in addition to those involved in formation of the 6,9-hemiacetal and/or 9,12-hemiacetal. The 9-ketone has both free C6 and C12 hydroxys. The 9,12-hemiacetal has a free C6 hydroxy (no C12 hydroxy), and the 6,9-hemiacetal has a free C12 hydroxy (no C6 hydroxy). A free C9 hydroxy is on both the 9,12- and 6,9-hemiacetals but not on the ketone. Thus, since a β-^{2}H shift is not seen on C9, the 9-ketone must be the major tautomer. The β-^{2}H shift on C6 (C6*) is about 75% of the total C6 signal, and the β-^{2}H shift on C12 (C12*) is about 50% of the total C12 signal. One would expect the same increase in the β-^{2}H shift at C6 and C12 due to the presence of the ketone C6 and C12 free hydroxys. Since the intensity of the β-^{2}H shift on C6 is greater than on C12, there must be more of the 9,12-hemiacetal than the 6,9-hemiacetal. These β-^{2}H shift findings are consistent with the ^{1}H NMR results which showed a 5 : 1 ratio of 9-ketone to 9,12-hemiacetal with a much lesser amount of the 6,9-hemiacetal.

Integration of protons on C11 with chemical shifts at 3.74 ppm for the ketone and 3.96 ppm for the 9,12-hemiacetal, indicates that the ketone to 9,12-hemiacetal ratio is approximately 5 : 1 in 90% H_2O and 10% ^2H_2O, at physiological pH. This is consistent with Barber *et al.*[11] for **1** in [$^2H_6$]DMSO compared to 5 : 2 in ^2H_2O. The ratio of the tautomers depends on factors such as temperature and solvent polarity.

This is the first structural investigation of **1** to be completed in 90% H_2O. Previously, a study was completed in ^2H_2O by Barber *et al.*[11] There were major differences in some chemical shifts between the present work and Barber *et al.*[11] For the 9-ketone there are differences for protons on C6OH, C12OH, C10, C7′8′, C2a″, C4″ and C6″. For the 9,12-hemiacetal there are different chemical shifts for protons on C8, C16, C21, C4e′ and C7′8′. The differences in chemical shifts are mostly attributable to a large difference in temperature and other experimental conditions. The present work was completed at room temperature (22 °C) while Barber *et al.*[11] completed their studies at 50 °C.

The present work supports the findings of Everett *et al.*[5] that the aglycone ring of **1** is primarily 'folded out' (type A aglycone

conformation) indicating that C4 is closer in conformational space to C11. This is in contrast to all of the derivative studies[14,16–18] previously mentioned which formed the 'folded in' (type B) conformation.

In a recent paper, Awan *et al.*[25] found the structure of azithromycin (**4**), in ^2H_2O at an apparent pH of 7.5 to be folded out compared to previous work in $C[^2H]Cl_3$, where it was folded in. This change to folded out in more polar solvents has been discussed by Lazarevski *et al.*[24] Awan *et al.*[25] also found **2** to exist in the folded out form in ^2H_2O, as did the 9-ketone of **1**. Awan *et al.*[25] found the two sugars in the up–up position for azithromycin in ^2H_2O, at apparent pH 7.5, as was the case in the present work for **1**.

In transfer NOE derived structures for **2**, **4** and **1**, weakly bound to bacterial ribosomes, conformational homology was found by Awan *et al.*,[25] in the C2–C6 region and desosamine sugar, but significant conformational differences were seen for the cladinose moiety. This variation led these authors to conclude that the C3 cladinose sugar was not required for the activity of **1**, whereas the C5 desosamine sugar was essential. It has long been believed that sugars interact in the cell at many sites. The activity of **1** is related to the ability of the ketone to bind to the 50S subunit of the 70S bacterial ribosome. This binding action inhibits protein synthesis.[15] The study of the conformation of the sugar moieties is thus important, as the sugars may play a role in the binding to the bacterial ribosome. The current study has determined the sugars for the 9-ketone to be in the boat conformation whereas Everett and Tyler[4] (as ascertained from their NOE data) and Gharbi-Benarous *et al.*[18,23] indicate that the sugars are in the chair conformation in deuterochloroform. As for findings in ^2H_2O by Barber *et al.*,[11] no information is discernible about the conformation of the sugars. The present work used NMR derived NOE constraints in the attainment of the conformational averages shown in Figs. 6 and 7.

In a molecular dynamics and NMR study in $C[^2H]Cl_3$ of **1** and **3** and their derivatives on the induction of hepatic cytochrome P-450, Gharbi-Benarous *et al.*[23] found four sugar conformers of **1** (2a, b, c and d in their Fig. 1). Using the definitions of $\Psi_1,\Psi_2,\Psi_3,\Psi_4$ given in the work by Gharbi-Benarous *et al.*,[23] the present study finds, for the 5 lowest energy structures of the 25 submitted for structure determination of the 9-ketone, the following average values for **1**: $\Psi_1 = -33.72$, $\Psi_2 = -29.09$, $\Psi_3 = -55.31$ and $\Psi_4 = -124.7°$. This compares to the four conformers of **2** found by Gharbi-Benarous *et al.*:[23] a: $\Psi_1 = 16$, $\Psi_2 = 40$, $\Psi_3 = 26$ and $\Psi_4 = 45°$; b: $\Psi_1 = 9$, $\Psi_2 = 60$, $\Psi_3 = 30$ and $\Psi_4 = 50°$; c: $\Psi_1 = -25$, $\Psi_2 = 5$, $\Psi_3 = 20$ and $\Psi_4 = 35°$; and d: $\Psi_1 = 12$, $\Psi_2 = 50$, $\Psi_3 = -30$ and $\Psi_4 = 5°$. Thus, in the structure determined by the present work the cladinose sugar is closer to the aglycone ring in the up position than in the study by Gharbi-Benarous *et al.*[23] The same is true for the desosamine sugar.

Everett and Tyler[4] studied **1** in deuterochloroform, and they found that there were small dipolar couplings between the ^1H atoms on C10 and C7a, C8 and C18, C8 and C19, C8 and C7e, C1′ and C18, and also C2′ and C4′a; medium couplings were found between the ^1H atoms on C11 and C4, C1′ and C5, C3 and C5, C7′8′ and C4′a, and C1′ and C5″ as well as large couplings between ^1H atoms on C7′8′ and C2′. All of the aforementioned NOE connectivities are consistent with the findings in this study. Everett and Tyler[4] also determined that large dipolar NOE couplings existed between the ^1H atoms on C1′ and C3 and C18 and C5. The results of the present work show the existence of medium couplings between these protons. This implies that these protons are farther apart in aqueous medium than in deuterochloroform. Everett and Tyler[4] determined that a medium dipolar (NOE) coupling existed between the ^1H atoms on C13 and C14e, C13 and C15 and C14a and C15. The present study found these couplings to be small. Everett and Tyler[4] found small couplings between the ^1H atoms on C2 and C16, C5′ and C6′, C2 and C17, C4″ and C7″ while the results of the present work showed these couplings to be large. The couplings between the ^1H atoms on C4 and C17, C7″ and C2″e and C2″a and C2″e were determined to be small by Everett and Tyler.[4] The present study determined these couplings to be of medium intensity implying a closer proximity in water.

Everett and Tyler[4] did not distinguish between the NMR parameters of the two major tautomers of **1** (9-ketone and 9,12-hemiacetal) as was done in the present study. They determined that there were small dipolar couplings between the ^1H atoms on C10 and C20 and that there were medium couplings between ^1H atoms on C1′ and C5. These through space couplings are consistent with the findings of this study except that these couplings are from the hemiacetal and not the ketone. Everett and Tyler[4] also determined that there were small NOE connectivities between the ^1H atoms on C11 and C3, C1″ and C2″e, and C2″a and C4″. This study determined the NOE couplings for these groups to be medium rather than strong and they existed on the hemiacetal and not the ketone.

The present study found large NOE couplings between ^1H atoms on C12OH and C2′, C6′ and C5, C16 and C10, C17 and C10, C3 and C4′a, C4′a and C2″e; medium couplings from ^1H atoms on C7′8′ and C7e, C7″ and C1″, C10 and C3, C14a and C7e as well as small couplings on C2″e and C7a, C17 and C1″, C4 and C7a, C6OH and C13, C13 and C3, C10 and C18, C18 and C14a, C18 and C7a, and C8 and C4′a. The study completed by Everett and Tyler[4] did not find any NOE couplings between these aforementioned ^1H atoms.

For the macrolide ring, the $^3J_{4-5}$ coupling of 6.9 Hz (Table 3) is consistent with the findings by Egan *et al.*[20] on diacetates or triacetates obtained for erythronolide B and 6-deoxyerythronolide B with acetylation of, respectively, the 3- and 5- and 3-,5- and 11-hydroxy groups. That the 3 and 5 diacetates or triacetates had a larger $^3J_{4-5}$ value than erythronolide B was explained by Egan *et al.*[20] on the basis of the 3 and 5 oxygen atoms moving apart by a rotation of the 4–5 bond such that the 5 oxygen is moved 'down'. In the present work, the cladinose and desosamine sugar moieties were parallel up at, respectively, the 3 and 5 positions of the agylcone ring. The 'extreme' (see reference 20 for a definition) $^3J_{7a-8}$ and $^3J_{7e-8}$ coupling constants of, respectively 9.7 and 3.8 Hz for the 9-ketone found in the present study, are consistent with findings of Egan *et al.*[20] in $C[^2H]Cl_3$ for the 3-acetyl, 5-acetyl and 3,5-diacetyl derivatives of erythronolide B corresponding to the totally staggered Perun conformation[21] with large $^3J_{7a-8}$ and small $^3J_{7e-8}$ coupling constants. The 2.69 ppm chemical shift of H8 (Table 1) correlates well with the 'extreme' coupling constants for the staggered Newman projection as per Egan *et al.*[20] Small $^3J_{7e-8}$ and large $^3J_{7a-8}$ coupling constants arise from interactions between protons at dihedral angles of about 180° (H7a to H8) and 60° (H7e to H8) as in the fully staggered Perun conformation. The dihedral angles found in the present study, respectively, for H7a to H8 and H7e to H8 were 173 and −78°. These values are consistent with Egan *et al.*[20] for the fully staggered Perun structure.

Thus, the 2.69 ppm chemical shift of H8 for the 9-ketone is consistent with the 'Perun' structure of the aglycone ring as in Egan *et al.*[20] However, the difference in coupling constant $^3J_{7a-8}$ of about 2 Hz between the present work and that of Everett and Tyler[4] is perplexing in view of the finding by Egan *et al.*[20] that a large $^3J_{7e-8}$ (11.5 Hz) tends to correlate with a large H8 chemical shift (3.30 ppm) characteristic of a partially eclipsed conformation *via* an 'outward' displacement of C7, decreasing the angle between H7a and H8, while that between H7e and H8 also decreases until, at the limit, the dihedral angles in the Newman projection, shown by Egan *et al.*,[20] are 120 and 0°. The chemical shift of H8 reported by Everett and Tyler[3] in $C[^2H]Cl_3$ is 2.68 ppm, consistent with the present work, but the magnitude of the $^3J_{7a-8}$ of 11.7 Hz (not $^3J_{7e-8}$) seen by Everett and Tyler[3] is more like the 'opposite extreme' $^3J_{7e-8}$ value of 11.5 Hz seen by Egan *et al.*[20] The $^3J_{7a-8}$ and $^3J_{7e-8}$ values reported by Everett and

Tyler[4] are not consistent with a fully staggered Perun type conformation for the aglycone ring, as described by Egan *et al.*[20] and as found in the present work. The same is true in comparing the coupling constants in the present work to those of Gharbi-Benarous *et al.*[23] in Table 3.

Everett *et al.*[5] have presented $^3J_{4-5}$, $^3J_{2-3}$ and selected chemical shifts reflecting the aglycone conformational blend for erythromycin derivatives in C[^{2}H]Cl$_3$. Conformation A generally occurs when a NOE is seen between protons on carbons 4 and 11. Conformation B generally occurs when a NOE is seen between protons on carbons 3 and 11. In the present study, medium intensity NOE connectivities were seen between protons on carbon 3 and 11 and large intensity NOE connectivities between protons on carbons 4 and 11. The observation of both 3 and 11 and 4 and 11 NOE connectivities has been interpreted[3–6] as indicating fast equilibration between conformations A and B of the aglycone ring. Everett *et al.*,[5] in a conformational study of erythromycin A in C[^{2}H]Cl$_3$ found this antibiotic to exist mainly in the type A conformation as reflected by a large [11]4 NOE and small [11]3 NOE. The present study with the NOE constraints used in the molecular modelling found the macrolide ring of the 9-ketone to be 'folded out' in the C3–C5 region (the mean H4 to H11 distance was found to be 1.96 Å) and to be flexible in the C6 to C9 region. The same results were obtained for the 9,12-hemiacetal. However, a fast equilibrium between the type A and type B aglycone conformers cannot be ruled out.

In the present study, differences were seen in the conformation of the sugar moieties for erythromycin A, boat forms being found, rather than chair forms, as in all past literature.[4,17,18,23] The sugar moieties are key to binding to the ribosomes, thus correct 3D structures of these moieties are essential. The finding of the sugars in the boat conformation is a major difference compared to past work in ^2H_2O *vs.* H_2O or *vs.* C[^{2}H]Cl$_3$. The polarity of ^2H_2O *vs.* H_2O should not change significantly, but the presence of NOEs not seen in other deuterated media compared to our results in H_2O are significant, leading to differences in sugar conformations compared to past findings. The choice of 90% water as the solvent allows one to see protons (6OH and 12OH were seen in the present study) that would not otherwise be seen due to rapid exchange with deuterium as would be the case in ^2H_2O (Barber *et. al.*[11]). The goal here was to complement findings in other solvents.

Experimental

For the ^{1}H NMR studies, erythromycin A (**1**) was prepared (0.7 mL in a 5 mm diameter NMR tube) to a final concentration of 10 mM in phosphate buffer at pH = 7.0 in 90% water and 10% deuterium oxide. The sample was degassed with argon. All NMR spectra were acquired at 22 °C on a Varian INOVA 400 spectrometer operating at 400.11 MHz for ^{1}H. The 1D proton spectrum was acquired with a spectral width of 9006 Hz, an acquisition time of 0.398 s, 8 transients and zero filling to 8k (32k for $^3J_{H-H}$ measurements) data points. The water peak was referenced to 4.75 ppm. All NMR data, unless otherwise stated, were acquired with presaturation of the water peak with a γH2 of 50 Hz and with digital oversampling. $^3J_{H-H}$ coupling constants (Table 3) were measured directly from the 1D ^{1}H NMR spectrum, after zero filling to 32k.

A 1D NOE difference spectrum of **1** was acquired with a *Z*-axis gradient triple-resonance probe using a recently published pulse sequence by Stott *et al.*[26] Water presaturation (γH2 = 55 Hz) and *Z*-gradient selection for water suppression were used with a shaped pulse for selective excitation of the proton on C5″ of the cladinose sugar unit of erythromycin A at 4.12/4.07 ppm (ketone/hemiacetal). The VNMR subroutine, 'Pandora's Box', was used to select the target multiplet and the optimum pulse shape/bandwidth (γH2 = 25 Hz) for the selective excitation pulse. In addition to the need to selectively excite a peak close to water with solvent suppression, erythromycin A poses the added challenge that all of the peaks in the ^{1}H NMR spectrum are upfield of 5.2 ppm, so that setting the transmitter on water requires some additional flexibility in acquisition and processing.

A homonuclear ^{1}H *z*-gradient DQFCOSY[27] spectrum was acquired with a spectral window of 9006 Hz in t2 and 2503 Hz in t1. For each of the 1024 t1 increments, 2 scans were signal averaged. A shifted sine-bell weighting function was applied along t1 and a Gaussian weighting function along t2.

The 2D-ROESY[28,29] and TOCSY[29,30] spectra were acquired with, respectively, mixing times of 200 ms and 60 ms. Previously recorded ROE buildup curves indicated that no significant spin diffusion occurs for aqueous erythromycin at a mixing time of 200 ms.

A spectral window of 9006 Hz was used in the detection domain and 2780 Hz in the evolution domain with an acquisition time of 0.205 s, and 2048 data points in the detection domain. For each of the 256 increments in t1, 4 transients were acquired. A γH2 of 2000 Hz was used for the ROESY spin-lock and 10 000 Hz for the clean TOCSY spin lock. The data was zero filled to 512 points in t1. A shifted sine-bell weighting function was applied along t1 with a Gaussian weighting function along t2. All of the 2D NMR spectra were acquired using hyper complex phase cycling[31] for phase-sensitive 2D.

^{13}C β-^{2}H spectra of **1** in 20 : 80 (293 600 scans) and 80 : 20 (305 456 scans) ^2H_2O : H_2O were acquired with WALTZ decoupling (with NOE) at 100.579 MHz using a 30° pulse, a spectral window of 25 000 Hz, an acquisition time of 0.328 s and a relaxation delay of 0.5 s. The spectra were processed with a line broadening of 2 Hz. All ^{13}C spectra were referenced to DSS§ at 0 ppm. The concentration of erythromycin was 8 mM (0.7 mL in a 5 mm diameter NMR tube) for all ^{13}C studies. The samples were prepared as for the ^{1}H NMR studies.

Molecular modelling of the 9-ketone and the 9,12-hemiacetal of **1** was carried out on a Silicon Graphics Indigo R4000 workstation using software purchased from Molecular Simulations Inc. (INSIGHT II, DISCOVER, NMR REFINE). Molecular structures were first optimized using the conjugate gradients energy minimization technique,[32] with a gradient convergence of 0.001 Å and an iteration limit of 1000 using the cff 91 force field.[33] NMR constraints (NOE distance ranges) were then introduced in each structure and 25 NMR structures for each molecule were calculated by distance geometry (DG II),[34] followed by simulated annealing[32] and energy minimization.[32] Final structures with the lowest number of constraint violations and with the lowest energies were retained.

A long range ^{13}C {^{1}H} HETCOR[35,36] of the sample used in Fig. 8(b) was acquired at 22 °C with a spectral window of 25 000 Hz, 4096 data points, and 2688 scans in the (^{13}C) detection domain. A spectral window of 9006 Hz with 64 increments in the evolution domain were used with sine bell weighting functions in t1 and t2. A bi-linear rotational decoupler (BIRD) pulse was employed during decoupling to decrease the intensity of directly bonded correlations.

§ 3-(Trimethylsilyl)-1-propanesulfonic acid, sodium salt.

References

1 J. M. McGuire, R. Bunch, H. E. Boaz, E. H. Flynn, H. M. Powell and J. W. Smith, *Antibiot. Chemother.*, 1952, **2,** 281.
2 J. A. Washington and W. R. Wilson, *Mayo Clin. Proc.*, 1985, **60**, 189.
3 J. R. Everett and J. W. Tyler, *J. Chem. Soc.*, *Perkin Trans. 2*, 1985, 2599.
4 J. R. Everett and J. W. Tyler, *J. Chem. Soc.*, *Perkin Trans. 2*, 1987, 1659.
5 J. R. Everett, I. K. Hatton and J. W. Tyler, *Magn. Reson. Chem.*, 1989, **28**, 1241.
6 J. R. Everett, E. Hunt and J. W. Tyler, *J. Chem. Soc.*, *Perkin Trans. 2*, 1991, 1481.
7 D. J. Ager and C. K. Sood, *Magn. Reson. Chem.*, 1987, **25**, 948.

8 D. M. Doddrell, D. T. Pegg and M. R. Bendall, *J. Magn. Reson.*, 1982, **48**, 323.
9 M. R. Bendall and D. T. Pegg, *J. Magn. Reson.*, 1983, **53**, 272.
10 A. Bax, R. Freeman, T. A. Frenkiel and M. H. Levitt, *J. Magn. Reson.*, 1981, **43**, 478.
11 J. Barber, J. I. Gyi, L. Lian, G. A. Morris, D. A. Pye and J. K. Sutherland, *J. Chem. Soc.*, *Perkin Trans. 2,* 1991, 1489.
12 P. E. Pfeffer, K. M. Valentine and F. W. Parrish, *J. Am. Chem. Soc.*, 1979, **101**, 1265.
13 J. C. Christofides and D. B. Davies, *J. Am. Chem. Soc.*, 1983, **83**, 5099.
14 W. E. Steinmetz, R. Bersch, J. Towson and D. Pesiri, *J. Med. Chem.*, 1992, **35**, 4842.
15 J. Majer, *Antimicrob. Agents Chemother.*, 1981, **19**, 628.
16 A. Awan, J. Barber, R. J. Brennan and J. A. Parkinson, *Magn. Reson. Chem.*, 1992, **30**, 1241.
17 J. Gharbi-Benarous, M. Delaforge and J. Girault, *Magn. Reson. Chem.*, 1990, **26**, 846.
18 J. Gharbi-Benarous, M. Delaforge, C. K. Jankowski and J. Girault, *J. Med. Chem.*, 1991, **34**, 1117.
19 J. F. Chantot, A. Bryskier and J. C. Gasc, *J. Antibiotics*, 1986, **39**, 660.
20 R. S. Egan, J. R. Martin, T. J. Perun and L. A. Mitscher, *J. Am. Chem. Soc.*, 1975, **97**, 4578.
21 T. J. Perun and R. S. Egan, *Tetrahedron Lett.*, 1969, 387.
22 D. Marion, M. Ikura, R. Tschudin and A. Bax, *J. Magn. Reson.*, 1989, **85**, 393.
23 J. Gharbi-Benarous, P. Ladam, M. Delaforge and J. Girault, *J. Chem. Soc.*, *Perkin Trans. 2*, 1993, 2303.
24 G. Lazarevski, M. Vinkovic, G. Kobrehei and S. Dokic, *Tetrahedron*, 1993, **49**, 721.
25 A. Awan, R. J. Brennan and J. Barber, *J. Chem. Soc.*, *Chem. Commun.*, 1995, 1653.
26 K. Stott, J. Keeler, Q. N. Van and A. J. Shaka, *J. Magn. Reson.*, 1997, **125**, 302.
27 O. W. Sorenson, G. W. Eich, M. H. Levitt, G. Bodenhausen and R. R. Ernst, *Progr. NMR Spectrosc.*, 1983, **16**, 163.
28 A. A. Bothner-By, R. L. Stephens, J. Lee, C. D. Warren and R. W. Jeanloz, *J. Am. Chem. Soc.*, 1984, **106**, 811.
29 A. Bax and D. G. Davis, *J. Magn. Reson.*, 1985, **63**, 207.
30 L. Braunschweiler and R. R. Ernst, *J. Magn. Reson.*, 1983, **53,** 521.
31 D. J. States, R. A. Haberkorn and D. J. Ruben, *J. Magn. Reson.*, 1982, **48**, 286.
32 M. J. D. Powell, *Math Program*, 1977, 251.
33 U. Dinur and A. T. Hagler, in Review of Computational Chemistry, ch. 4, ed. K. B. Lipkowitz and D. B. Boyd, VCH, New York, 1991.
34 G. M. Crippen and T. F. Havel, *Distance Geometry and Molecular Conformation*, Research Studies Press, New York, 1988.
35 G. Martin, *Magn. Reson. Chem.*, 1988, **26**, 28.
36 V. V. Krishnamurthy, *J. Magn. Reson.*, 1988, **80**, 280.

Paper 8/02865F
Received 16*th April* 1998
Accepted 12*th June* 1998